

The object of research is the process that forms an elliptical directional diagram of the H-sector horn antenna for flow irradiation of seeds with the electromagnetic field.

The emitter of electromagnetic energy is presented as one of the main elements of installations for irradiating seeds with an electromagnetic field before sowing. This parameter was investigated by taking into account the values of the biotropic parameters of the low-energy electromagnetic field under the conditions of flow processing.

This paper reports a study into the parameters of the H-sector horn emitter for irradiation of sugar beet seeds with a low-energy electromagnetic field at a frequency of 73...75 GHz in continuous flow. Thus, one should use the H-sectoral horn emitter with the following parameters: aperture width  $aa=20$  mm; horn length  $R_H=35$  mm;  $b=1.8$  mm. It is determined that in order to irradiate sugar beet seeds on the conveyor plane with a power flow density of  $P=100 \mu\text{W}/\text{cm}^2$ , it is necessary to place two horns 1200 mm above the conveyor at a distance of 2540 mm from each other. It was checked that the treatment of sugar beet seeds with electromagnetic radiation in a continuous flow with a capacity of 300 kg/h is possible with a power of up to 2 W supplied to two horn antennas; the speed of the conveyor is 15 cm/s.

The parameters of the sectoral horn for an elliptical directional diagram were studied by dividing the main task into internal and external.

According to the results of the research, it is possible to build a base of geometric presets for adjusting installations for different types of seeds, the desired performance, the structural features of installations, as well as existing emitters

**Keywords:** low-energy electromagnetic radiation, electromagnetic field emitter, horn antenna, H-sectoral antenna, directional diagram, sugar beet seeds, presowing treatment

UDC 537.8: 631.53.027.34:633.63

DOI: 10.15587/1729-4061.2023.273972

# FORMING AN ELLIPTICAL DIRECTIONAL DIAGRAM OF THE SECTORAL HORN ANTENNA FOR FLOW IRRADIATION OF SUGAR BEET SEEDS BY ELECTROMAGNETIC FIELD

**Natalia Kosulina**

Corresponding author

Doctor of Technical Sciences, Professor\*

E-mail: kosnatgen@ukr.net

**Maksym Sorokin**

PhD\*

**Yuri Handola**

PhD\*

**Stanislav Kosulin**

Department of Oncosurgery, Radiation Therapy and Palliative Care

Kharkiv Medical Academy of Postgraduate Education

Amosova str., 58, Kharkiv, Ukraine, 610176

**Kostiantyn Korshunov**

Postgraduate Student\*

\*Department of Electromechanics, Robotics, Biomedical Engineering and Electrical Engineering

State Biotechnological University

Alchevskykh str., 44, Kharkiv, Ukraine, 61002

Received date 07.12.2022

Accepted date 12.02.2023

Published date 28.02.2023

**How to Cite:** Kosulina, N., Sorokin, M., Handola, Y., Kosulin, S., Korshunov, K. (2023). Forming an elliptical directional diagram of the sectoral horn antenna for flow irradiation of sugar beet seeds by electromagnetic field. *Eastern-European Journal of Enterprise Technologies*, 1 (5 (121)), 26–37. doi: <https://doi.org/10.15587/1729-4061.2023.273972>

## 1. Introduction

Increasing the yield and sugar content of sugar beet root crops is considered the main direction of agricultural production [1–3]. Traditional ways to increase the yield of sugar beet are associated with the use of high agricultural technology, the use of fertilizers, irrigation, chemical and biological means of protection, and achievements of genetics and biotechnology. It is not possible to fully implement the listed means to increase the yield and sugar content of sugar beet root crops due to their complexity and energy intensity, the complexity of application, and environmental safety [4–6].

Studies on the effect of high-frequency (HF), ultra-high frequency (UHF), and super-high frequency (SHF) EMF on seeds of different crops show that they, under certain energy-information parameters of EMF, can increase germination and germination energy by up to 30 %. Plants grown from processed seeds of UHF and SHF ranges of EMF sprout a few days earlier than the control, have an advantage

in vegetative mass and yield up to 30–40 %; substandard seeds reach the level of conditioned [7, 8].

To obtain useful changes in a biological object, it is necessary to find such a structure of external EMF (frequency, power, exposure, polarization), which would lead to the desired effect [9, 10]. For example, increasing yields and breeding new varieties of grain and vegetable crops, treating animals, combating harmful insects in agriculture [11, 12].

New research confirms the concept of the wave nature of gene information transmission [13, 14]. The simplest model of a cell membrane is a combination of a large number of elementary auto generators (oscillators) that are interconnected. Within each group, individual auto generators either oscillate independently of each other or are mutually synchronized. This is possible if the connection between them is weak, and the alignment of their natural frequencies is too large.

A characteristic feature of the phenomenon of synchronization of self-oscillations is the low power required for syn-

chronization of an external signal, the limit value of which depends on the noise level in the system and the variation of partial frequencies of individual auto generators. For real bio-objects, the threshold value naturally depends on the depth of the resonating structures relative to the surface subjected to electromagnetic radiation, and on the intensity of absorption of electromagnetic waves in near surface-located tissues. The increase in the power of the external signal above the threshold does not make qualitative changes in the nature of the synchronized oscillations [15, 16].

The magnitude of the EMF power flow density for real crop production objects depends on the specific mechanisms of influence of the external field. The noise level in biological objects should not exceed the level of weak non-covalent relationships in a micro-object: ionic interactions, hydrogen bonds, and Van der Waals ties. With the help of these connections, information is realized that fits into the sequence of macromolecular chains [17, 18].

Practical energy levels to influence plant seeds should be units – tens of  $\mu\text{W}/\text{cm}^2$ . For seed treatment, installations with the following parameters are required: productivity, 300 kg/hour; frequency, 73...75 GHz; power flow density, 95...100  $\mu\text{W}/\text{cm}^2$ ; exposure, 32...34 s [8, 19, 20].

Effective use of low-energy EMF of the SHF range is impossible without the construction of antennas for appropriate electromagnetic radiation and the use of devices for finding optimal technological parameters of EMF.

Studies on determining the parameters of the antenna (emitter) of electromagnetic energy with an elliptical directional diagram for flow seed processing are relevant since they will allow more efficient use of the influence of the information electromagnetic field of the super-high frequency range (SHF) in agricultural production.

---

## 2. Literature review and problem statement

---

Considering the designs of existing seed production plants, it can be noted that most of them are not meant for low-energy processing. The remaining few installations have either a high cost or are intended for the cultivation of only one type of seed [8, 19, 21, 22].

Reducing the cost and ensuring universality can be carried out by viewing the choice of the emitter with the study of its parameters in relation to the tasks of flow processing.

As can be seen from [23], one of the main elements of the installation for presowing seed treatment is the emitter of electromagnetic energy. It forms the necessary directional diagram [24, 25] and provides a sufficient level of power flow density on the seeds when the conveyor belt is moving.

In the SHF wavelength range, various types of antennas are widely used: wave-slit (first type) [26], surface wave antennas (second type) [27], horn (third type) [28], banded [29], and others [30].

Wave-slit antennas obtained by cutting gaps in waveguide systems are a type of linear multi-element antennas. They provide a narrowing of the directional diagram (DD) in the plane passing through the axis of the waveguide. There are resonant and non-resonance antennas, as well as antennas with coordinated slits [29, 30]. For antennas of the first type, the distance between adjacent slits  $d$  is equal to the waveguide wavelength ( $\lambda_x$ ). In antennas with coordinated slits, each slit is separately coordinated with the waveguide using a jet vibrator or diaphragm [26]. In a sepa-

rate case, the length of the slits is  $\lambda/2$  ( $\lambda$  is the wavelength in free space), and their width  $d_1=(0.05..0.1)\lambda$ . It is clear then that the use of this type of antenna in the wavelength range  $<7$  mm is quite problematic. The cross section of the single-mode waveguide rectangle in this range is  $3.6\times 1.8$  mm. The disadvantage of wave-slit, as well as banded antennas, are rather limited range properties. When the frequency changes in such antennas, DD deviates in space from a given direction [29], which is accompanied by a change in its width while the alignment of the antenna with the supply waveguide also changes.

The use of surface wave antennas [27] will avoid the above disadvantages. This class includes antennas with a slow phase velocity ( $V_p < c$ ). Antennas of this type are distinguished by the structure that slows down the phase speed. A distinctive feature of a wave with  $V_p < c$  is a decrease in the amplitude of the wave field at a distance from the slow-down structure according to the exponential law. Moreover, the rate of decrease is greater, the greater the deceleration of the wave.

Therefore, a characteristic feature of such antennas is their small transverse dimensions. As flat deceleration systems, comb structures and structures are used in the form of a thin layer of dielectric on a metal substrate. If we consider the comb as a decelerating structure, then the following conditions must be met for it: the period  $D \leq 0.1\lambda$ ; the depth of the grooves  $h$  must be less than  $\lambda/4$ . From here it becomes clear what geometric dimensions the comb should have in the four-millimeter wavelength range and what is the expected cost of its manufacture. On the other hand, it is necessary to ensure the effective excitation of the decelerating structure without the appearance of higher types of waves and reflections. This is a complex technical task. The disadvantages of surface wave antennas include relatively small realized amplification and a relatively high level of side petals. In accordance with the above, we can conclude that the use of antennas of a similar type to solve the tasks set is not rational.

In works [28, 31], the results of studies of wave-horn antennas are given. It is shown that the advantages of a wave-horn antenna, unlike those discussed above, are broadband devices that provide about one and a half overlap in the range. They are easy to manufacture. In general, the horn is a wave transformer propagating through the supply waveguide, into a wave of the second type.

There is a transformation of a flat wave of small size in the cross section of the waveguide into an approximately flat wave of impressive size into the aperture of the horn. In addition, due to the smooth change of wave resistance along the horn, the waveguide is coordinated with the free space. Accordingly, the reflection from the aperture is reduced.

There are conical, pyramidal, and sectoral emitters [28]. Conical horn antennas are built on the basis of a round waveguide, through which the main waveguide  $TE_{11}$  propagates. They have several disadvantages: the field polarization plane of such antennas is unstable and easily changes even with minor wall deformations; the field in the aperture of such an emitter at different points is polarized differently. In addition, the DD of such antennas has approximately axial symmetry.

Ensuring linear polarization of the irradiating field at the seed location and the need to be much narrower in width DD gave the basis to consider pyramidal [31] and sectoral horn antennas.

Emitters of this type are built on the basis of rectangular waveguide systems [31].

In [31] it is noted that pyramidal antennas are used, as a rule, to obtain a narrow DD in two mutually perpendicular planes, the remaining.

In works [26–32] the issue of obtaining a broad DD remained unresolved.

In order to obtain a wide DD (which will make it possible to overlap the width of the conveyor tape), a sectoral horn emitter can be used, which is given in work [33].

In general, sectoral is such a horn, in which only one cross-sectional size of a rectangular waveguide increases, and the other remains unchanged. In this regard, there are the *H*-sector horn, with the expansion in the plane of the vector *H* of the main waveguide wave *TE*<sub>10</sub> and the *E*-sector horn, with an extension in the plane of the vector *E*. Reflection coefficient of the waveguide *TE*<sub>10</sub> from the articulation of the waveguide with the *H*-sector horn is less than in the case of the *E*-sectoral horn; it is necessary to consider the emitter with an extension in the plane of the vector *H*.

The emitter of electromagnetic energy should form the necessary directional diagram and ensure a sufficient level of power flow density on sugar beet seeds when moving a container tape at a speed of 10...15 cm/s.

All this will allow us to assert that it is expedient to conduct a study of the formation of an elliptical directional diagram of a sectoral horn antenna for flow irradiation of sugar beet seeds with a low-energy electromagnetic field before sowing.

### 3. The aim and objectives of the study

The aim of this study is to form an elliptical directional diagram of a sectoral horn antenna for flow irradiation of sugar beet seeds with a low-energy electromagnetic field before sowing. This will make it possible to ensure a sufficient level of power flow density on sugar beet seeds when the container tape is moving.

To accomplish the aim, the following tasks have been set:

- to determine the antenna parameters: width and aperture length of the *H*-sectoral horn emitter for electromagnetic field irradiation of sugar beet seeds in a continuous stream with a frequency of 73...75 GHz;
- to determine the flux density of the radiation power of the electromagnetic field, the height of placement above the conveyor plane, the number of emitter horns and their location;
- to determine the required power supplied to the irradiator horn and the speed of the conveyor.

## 4. Materials and research methods

### 4. 1. Object and hypothesis of research

The object of this study is the process of forming an elliptical directional diagram of a sectoral horn antenna for flow irradiation of seeds with an electromagnetic field.

The research hypothesis is the interaction of the electromagnetic field with sugar beet seeds.

Simplifications and assumptions are accepted: in the horn throughout there is only the main type of wave; reflection from the aperture does not lead to the emergence of higher types of waves; the amplitude distribution of the field

in the horn aperture repeats the distribution of the field in the cross section of the feed waveguide; horn walls are considered ideally conducting.

### 4. 2. Internal problem for the *H*-sectoral horn

It is necessary to conduct research by dividing the main problem into internal and external. Despite the connection between the field inside and outside the horn, the internal problem must be solved regardless of the external problem. The resulting field values in the extension plane of the *H*-sectoral horn can be used to solve an external problem. The directional diagram of the emitter, according to the known distribution of the field in the aperture of the horn, was calculated by wave optics based on the Huygens principle and the Kirchhoff formula.

The amplitude distribution of the field in the aperture of the irradiator under consideration was taken the same as in the supply waveguide. The horn is excited by a rectangular waveguide through which the *TE*<sub>10</sub> wave propagates. Along the *x*-axis passing in the plane of the vector  $\vec{H}$ , the distribution of the amplitude of the field is cosine. Along the axis *y*, passing in the plane of the vector  $\vec{E}$ , the amplitude distribution is uniform. Due to the fact that the wave front in the horn does not remain flat but is transformed into cylindrical, during the analysis it is advisable to proceed to a cylindrical coordinate system *y*,  $\rho$ ,  $\phi$  (Fig. 1).

We put the horn infinitely long, and its walls are perfectly conductive. We also take into account that inside the horn  $\vec{j}_e$  and  $\vec{j}_m$  equal zero. These conditions mean that the sources of excitation of the electromagnetic field are outside the horn.

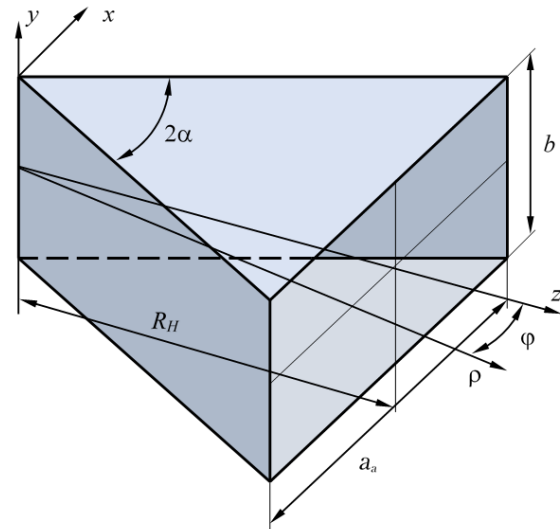


Fig. 1. Conditional image of the *H*-sectoral horn

In the *H*-sectoral horn, in which, as in a rectangular waveguide, mainly *TE*<sub>10</sub> wave propagates [29, 33, 34]:

$$E_y(\rho, \varphi) = C H_{\frac{\pi}{2\alpha}}^{(2)}(k\rho) \cos\left(\frac{\pi\varphi}{2\alpha}\right), \tag{1}$$

$$H_\rho(\rho, \varphi) = C \frac{\pi}{i\omega\mu_0 2\alpha\rho} H_{\frac{\pi}{2\alpha}}^{(2)}(k\rho) \sin\left(\frac{\pi\varphi}{2\alpha}\right), \tag{2}$$

$$H_\varphi(\rho, \varphi) = C \frac{k}{i\omega\mu_0} \left( \frac{d}{d(k\rho)} H_{\frac{\pi}{2\alpha}}^{(2)}(k\rho) \right) \cos\left(\frac{\pi\varphi}{2\alpha}\right). \tag{3}$$

The resulting ratios allow us to make a number of important comments. At great distances from the top of the horn, the EMF, which has the character of a cylindrical wave, is purely transverse (2), (3). This is due to the fact that in this case it is possible to neglect  $H_\rho(\rho, \phi)$  of the EMF component compared to  $H_\phi(\rho, \phi)$ . And this is possible with  $k \gg \pi/2\alpha\rho$  or  $k\rho \ll \pi/2\alpha$ . This inequality is the condition that allows replacing the Hankel function with its asymptotic approximation. If this condition is met, one can replace expression (1) to (3) with the following equations for the field's constituents:

$$E_y(\rho, \phi) = C \sqrt{\frac{2}{\pi k \rho}} \cos\left(\frac{\pi\phi}{2\alpha}\right) \exp\left[-ik\rho + i\left(\frac{\pi}{2\alpha} + \frac{1}{2}\right)\frac{\pi}{2}\right], \quad (4)$$

$$H_\phi(\rho, \phi) = E_y(\rho, \phi)/120\pi, \quad (5)$$

$$H_\rho = E_\phi = E_\rho = 0, \quad (6)$$

$$Z_{H_{10}} = Z_0 / \sqrt{1 - (\lambda/2a_a)^2}. \quad (7)$$

The resistivity of the  $H$ -sectoral horn decreases with increasing irradiator length, approaching the wave resistance of free space. Accordingly, the horn in question, in contrast to the rectangular waveguide, turns out to be an antenna that is well coordinated with free space. In addition, since the aperture of the antenna under consideration is flat, and the wave propagating through such an emitter is cylindrical, the field in the aperture will not be synphase, which as a result will lead to phase distortions.

To determine the phase distortions in the aperture of the  $H$ -sectoral horn, its cross-section in the  $xOz$  plane is considered (Fig. 2).

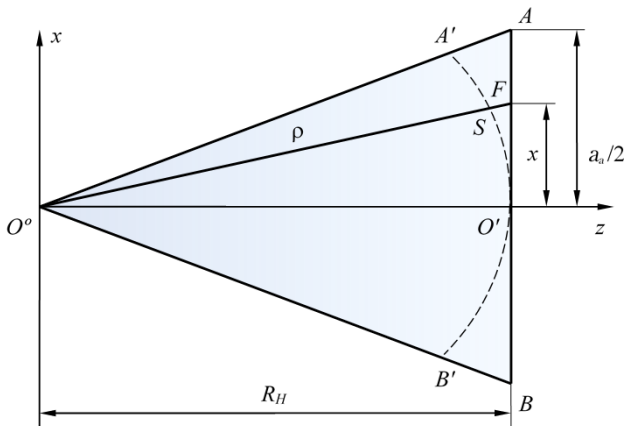


Fig. 2. Determining phase distortions in the horn aperture

In the case of the  $H$ -sectoral horns used in practice, the field in the aperture remains unexcited with relatively large cross-sectional dimensions, that is, it is equal to the field of the incoming wave [35, 36].

In Fig. 2 the longitudinal cross section of the horn is represented as a triangle. And since the phase front of the wave propagating through the horn in question forms a cylindrical surface, at different points of the aperture the phases of the field will be different. The  $OO'$  line is a line of constant phases of the field in this cross-section.

The phase distribution in expression (28) is defined as:

$$\Psi(\rho) = k\rho - \left(\frac{\pi}{2\alpha} + \frac{1}{2}\right)\frac{\pi}{2}, \quad (8)$$

and if at the point  $O'$  (the middle of the aperture) we take the phase of the field equal to zero, then (8) will take the form:

$$\Psi(R_\rho) = kR_\rho - \left(\frac{\pi}{2\alpha} + \frac{1}{2}\right)\frac{\pi}{2} = 2\pi n. \quad (9)$$

At an arbitrary point  $F$ , located on the axis of the aperture, at a distance  $x$  from the point  $O'$ , the phase of the field lags behind the phase in the middle of the aperture by a phase angle (Fig. 2):

$$\begin{aligned} \Delta\Psi &= \frac{2\pi}{\lambda}(OF - OO') = \frac{2\pi}{\lambda}(OF - R_H) = \\ &= \frac{2\pi R_H}{\lambda} \left( \sqrt{1 + \left(\frac{x}{R_H}\right)^2} - 1 \right). \end{aligned} \quad (10)$$

Since usually in horns the width of the aperture  $a_a$  is much less than the length  $R_H$ , the condition  $x \ll R_H$  can be applied to (10). Using the root decomposition by powers  $x/R_H$  and discarding terms above the second order, expression (10) can be rewritten as:

$$\Delta\Psi = \frac{2\pi R_H}{\lambda} \left( 1 + \frac{x^2}{2R_H^2} - \frac{x^4}{4R_H^4} + \dots - 1 \right) \approx \frac{\pi x^2}{\lambda R_H}. \quad (11)$$

According to Fig. 2,  $\rho = \sqrt{R_H^2 + x^2}$ , then, taking into account (9) and (11), expressions (4) and (5):

$$E_y(\rho, \phi) = E_0 \sqrt{\frac{R_H}{\sqrt{R_H^2 + x^2}}} \cos\left(\frac{\pi\phi}{2\alpha}\right) \exp\left[-i\frac{\pi x^2}{\lambda R_H}\right], \quad (12)$$

$$H_\phi(\rho, \phi) = E_y(\rho, \phi)/120\pi, \quad (13)$$

where  $E_0 = C \sqrt{2/\pi k R_H}$ .

Under the above condition  $x \ll R_H$ , in the case of calculating the radiation field, the following assumptions can be accepted [35, 36]:

$$\begin{cases} \frac{R_H}{\sqrt{R_H^2 + x^2}} \cong 1, \\ \frac{\phi}{2\alpha} \cong \frac{x}{a_p}, \\ H_\phi \cong -H_x, \end{cases} \quad (14)$$

where  $H_\phi$  is tangent to the curve  $A'O'B'$ , and  $H_x$  is parallel to the straight line  $AOB$ .

After substituting (14) into expressions (12) and (13), we obtained the resulting form of a ratio that defines the components of EMF in the  $H$ -sectoral horn aperture:

$$E_y(\rho, \phi) = E_0 \cos\left(\frac{\pi x}{a_a}\right) \exp\left[-i\frac{\pi x^2}{\lambda R_H}\right], \quad (15)$$

$$H_x(\rho, \phi) = -E_y(\rho, \phi)/120\pi, \quad (16)$$

where  $E_0 = C \sqrt{2/\pi k R_H}$ .

Determination of the electric and magnetic field strength (15), (16) makes it possible to determine the directional

function of the emission system of emitters  $E_{SG}(\theta_E)$  and find the phase of the field in the aperture of the  $H$ -sectoral horn. Subsequently, it is possible to analyze at what points the minimum and maximum value of phase delay will be and obtain the necessary ratios to determine the length of the sectoral horn in the vector plane.

**4. 3. External problem for the  $H$ -sectoral horn**

To determine the electric field strength of the  $H$ -sectoral horn in the far zone  $E_E(\theta_E)$ , the Bonch-Brujevic rule was used [37–39].

It was accepted that the value of the field strength of a single Huygens emitter in the far zone is known [39, 40]. Further, accordingly, to calculate the field of aperture in the same zone, it was represented as filled with continuously located Huygens emitters, the amplitude, phase, and direction of the currents of which are the same. Thus, to calculate the directional function of the system of identical and equally oriented emitters, the directional function of one emitter  $E_G(\theta_E)$  must be multiplied by the directional function of the emitter system  $E_{SG}(\theta_E)$  considered as non-directional [39, 40]:

$$E_E(\theta_E) = E_G(\theta_E)E_{SG}(\theta_E). \tag{17}$$

The value of  $E_{SG}(\theta_E)$  was found using expression (15) and the inverse Fourier transform. Then ratio (17) takes the form:

$$\begin{aligned} E_E(\theta_E) &= E_G(\theta_E) \times \\ &\times \int_{-a_e/2}^{a_e/2} \int_{-b/2}^{b/2} E_0 \cos\left(\frac{\pi x}{a_a}\right) \exp\left(-i\frac{\pi x^2}{\lambda R_H}\right) \exp(iky \sin\theta_E) dx dy = \\ &= E_G(\theta_E) \int_{-a_e/2}^{a_e/2} E_0 \cos\left(\frac{\pi x}{a_a}\right) \exp\left(-i\frac{\pi x^2}{\lambda R_H}\right) dx \times \\ &\times \int_{-b/2}^{b/2} \exp(iky \sin\theta_E) dy. \end{aligned} \tag{18}$$

After calculating the second integral in (18), we received:

$$E_E(\theta_E) = E_0 E_G(\theta_E) K_1 b \frac{\sin\left(\frac{\pi b}{\lambda} \sin\theta_E\right)}{\frac{\pi b}{\lambda} \sin\theta_E}, \tag{19}$$

where  $K_1 = \int_{-a_e/2}^{a_e/2} \cos\left(\frac{\pi x}{a_a}\right) \exp\left(-\frac{\pi x^2}{\lambda R_H}\right) dx$ .

This integral in the case of a cross section  $y0z$  ( $x=0$ ) is equal to  $a_a$ . At  $\theta_E=0^\circ$   $E_E^{\max}(0^\circ) = E_0 a_a b$ ,  $E_G(0^\circ) = 1$ .

After normalization of  $(F_E(\theta_E) = E_E(\theta_E) / E_E^{\max}(0^\circ))$ , the resulting form of the expression defining the DD of the  $H$ -sectoral horn in the  $y0z$  plane:

$$F_E(\theta_E) = F_G(\theta_E) \sin\left(\frac{\pi b}{\lambda} \sin\theta_E\right) / \frac{\pi b}{\lambda} \sin\theta_E, \tag{20}$$

where  $F_G(\theta_E) = E_G(\theta_E) / E_G(0^\circ) = (1 + \cos\theta_E) / 2$  is the normalized DD of a single Huygens emitter in the far zone [38].

From ratio (20), it follows that the directional diagram (DD) of the  $H$ -sectoral horn in the plane of the main wave vector  $\vec{E}$  in the rectangular waveguide  $TE_{10}$  coincides

with the DD of the open end of the rectangular waveguide in the same plane in the absence of a reflection in it ( $|K|=0$ ).

The electric field strength of the aperture in the far zone in the plane of the vector  $\vec{H}$  is equal to:

$$\begin{aligned} E_H(\theta_H) &= E_G(\theta_H) \times \\ &\times \int_{-a_e/2}^{a_e/2} \int_{-b/2}^{b/2} E_0 \cos\left(\frac{\pi x}{a_a}\right) \exp\left(-i\frac{\pi x^2}{\lambda R_H}\right) \exp(ikx \sin\theta_H) dx dy = \\ &= E_0 b E_G(\theta_H) \times \\ &\times \int_{-a_e/2}^{a_e/2} \cos\left(\frac{\pi x}{a_a}\right) \exp\left(-i\frac{\pi x^2}{\lambda R_H}\right) \exp(ikx \sin\theta_H) dx. \end{aligned} \tag{21}$$

We considered the integral in expression (21) separately. If we represent the trigonometric function in the following form [41]:

$$\cos(\pi x/a_a) = [\exp(i\pi x/a_a) + \exp(-i\pi x/a_a)]/2,$$

and enter the notation, then ratio (21) takes the form:

$$E_H(\theta_H) = E_0 b E_G(\theta_H) \frac{1}{2} \times \left\{ \begin{aligned} &\int_{-a_e/2}^{a_e/2} \exp\left(-i\frac{\pi x^2}{\lambda R_H}\right) \exp\left(i\frac{\pi x}{a_a}\right) \exp(ikx \sin\theta_H) dx + \\ &+ \int_{-a_e/2}^{a_e/2} \exp\left(-i\frac{\pi x^2}{\lambda R_H}\right) \exp\left(-i\frac{\pi x}{a_a}\right) \exp(ikx \sin\theta_H) dx \end{aligned} \right\}. \tag{22}$$

We analyzed the first integral in parentheses of ratio (22):

$$\begin{aligned} E_H^{(1)}(\theta_H) &= \\ &= \int_{-a_e/2}^{a_e/2} \exp\left(-i\frac{\pi x^2}{\lambda R_H}\right) \exp\left(i\frac{\pi x}{a_a}\right) \exp(ikx \sin\theta_H) dx = \\ &= \int_{-a_e/2}^{a_e/2} \exp\left\{-i\pi\left[\frac{x^2}{\lambda R_H} - x\left(\frac{1}{a_a} + \frac{2\sin\theta_H}{\lambda}\right)\right]\right\} dx. \end{aligned} \tag{23}$$

We converted the exponent's power indicator in (23):

$$\begin{aligned} &-i\pi\left[\frac{x^2}{\lambda R_H} - x\left(\frac{1}{a_a} + \frac{2\sin\theta_H}{\lambda}\right)\right] = \\ &= -\frac{i\pi}{2} \left\{ \left[ \frac{x\sqrt{2}}{\sqrt{\lambda R_H}} - \frac{\sqrt{\lambda R_H}}{\sqrt{2}} \left(\frac{1}{a_a} + \frac{2\sin\theta_H}{\lambda}\right) \right]^2 - \right. \\ &\left. - \frac{\lambda R_H}{2} \left(\frac{1}{a_a} + \frac{2\sin\theta_H}{\lambda}\right)^2 \right\}. \end{aligned} \tag{24}$$

And after entering a new variable

$$u = \left[ \frac{x\sqrt{2}}{\sqrt{\lambda R_H}} - \frac{\sqrt{\lambda R_H}}{\sqrt{2}} \left(\frac{1}{a_a} + \frac{2\sin\theta_H}{\lambda}\right) \right],$$

expression (23) takes the form:

$$E_H^{(1)}(\theta_H) = M \int_{-V_2}^{V_1} \exp\left(-i\frac{\pi}{2}u^2\right) du, \quad (25)$$

where  $M = \frac{\sqrt{\lambda R_H}}{\sqrt{2}} \exp\left[i\frac{\pi\lambda R_H}{4}\left(\frac{1}{a_a} + \frac{2\sin\theta_H}{\lambda}\right)^2\right]$ ,

$$V_1 = \frac{1}{\sqrt{2}} \left[ \frac{a_a}{\sqrt{\lambda R_H}} - \sqrt{\lambda R_H} \left( \frac{1}{a_a} + \frac{2\sin\theta_H}{\lambda} \right) \right],$$

$$V_2 = \frac{1}{\sqrt{2}} \left[ \frac{a_a}{\sqrt{\lambda R_H}} + \sqrt{\lambda R_H} \left( \frac{1}{a_a} + \frac{2\sin\theta_H}{\lambda} \right) \right].$$

$$\int_{-a}^0 f(x) dx = \int_0^a f(-x) dx, \quad (26)$$

then expression (25) takes the following form:

$$E_H^{(1)}(\theta_H) = M \left[ \int_0^{V_1} \exp\left(-i\frac{\pi}{2}u^2\right) du + \int_0^{V_2} \exp\left(-i\frac{\pi}{2}u^2\right) du \right]. \quad (27)$$

We considered the first integral in expression (27), which, taking into account the Euler formula [39], takes the form:

$$\int_0^{V_1} \exp\left(-i\frac{\pi}{2}u^2\right) du = \int_0^{V_1} \cos\left(\frac{\pi}{2}u^2\right) du - i \int_0^{V_1} \sin\left(\frac{\pi}{2}u^2\right) du. \quad (28)$$

Similarly, the second integral included in expression (27):

$$\int_0^{V_2} \exp\left(-i\frac{\pi}{2}u^2\right) du = \int_0^{V_2} \cos\left(\frac{\pi}{2}u^2\right) du - i \int_0^{V_2} \sin\left(\frac{\pi}{2}u^2\right) du. \quad (29)$$

The integrals included in ratios (28) and (29) are called the Fresnel integrals, defined as [40]:

$$C\left(\frac{\pi}{2}z^2\right) = \int_0^z \cos\left(\frac{\pi}{2}t^2\right) dt, \quad S\left(\frac{\pi}{2}z^2\right) = \int_0^z \sin\left(\frac{\pi}{2}t^2\right) dt. \quad (30)$$

The resulting form, taking into account ratios (4) to (6):

$$E_H^{(1)}(\theta_H) = M \left\{ \left[ C\left(\frac{\pi}{2}V_1^2\right) + C\left(\frac{\pi}{2}V_2^2\right) \right] - \left[ -i \left[ S\left(\frac{\pi}{2}V_1^2\right) + S\left(\frac{\pi}{2}V_2^2\right) \right] \right] \right\}. \quad (31)$$

We considered the second integral in parentheses in ratio (22):

$$\begin{aligned} E_H^{(2)}(\theta_H) &= \int_{-a_a/2}^{a_a/2} \exp\left(-i\frac{\pi x^2}{\lambda R_H}\right) \exp\left(-i\frac{\pi x}{a_a}\right) \exp(ikx\sin\theta_H) dx = \\ &= \int_{-a_a/2}^{a_a/2} \exp\left\{-i\pi \left[ \frac{x^2}{\lambda R_H} + x \left( \frac{1}{a_a} - \frac{2\sin\theta_H}{\lambda} \right) \right]\right\} dx. \end{aligned} \quad (32)$$

We converted the exponent's power indicator in equation (32):

$$\begin{aligned} &-i\pi \left[ \frac{x^2}{\lambda R_H} + x \left( \frac{1}{a_a} - \frac{2\sin\theta_H}{\lambda} \right) \right] = \\ &= -i\frac{\pi}{2} \left[ \left[ \frac{x\sqrt{2}}{\sqrt{\lambda R_H}} + \frac{\sqrt{\lambda R_H}}{\sqrt{2}} \left( \frac{1}{a_a} - \frac{2\sin\theta_H}{\lambda} \right) \right]^2 - \frac{\lambda R_H}{2} \left( \frac{1}{a_a} - \frac{2\sin\theta_H}{\lambda} \right)^2 \right]. \end{aligned} \quad (33)$$

After entering a new variable

$$\left[ \frac{x\sqrt{2}}{\sqrt{\lambda R_H}} + \frac{\sqrt{\lambda R_H}}{\sqrt{2}} \left( \frac{1}{a_a} - \frac{2\sin\theta_H}{\lambda} \right) \right] = g,$$

expression (32) takes the form:

$$E_H^{(2)}(\theta_H) = N \int_{-W_2}^{W_1} \exp\left(-i\frac{\pi}{2}g^2\right) dg, \quad (34)$$

where  $N = \frac{\sqrt{\lambda R_H}}{\sqrt{2}} \exp\left[i\frac{\pi\lambda R_H}{4}\left(\frac{1}{a_a} - \frac{2\sin\theta_H}{\lambda}\right)^2\right]$ ,

$$W_1 = \frac{1}{\sqrt{2}} \left[ \frac{a_a}{\sqrt{\lambda R_H}} + \sqrt{\lambda R_H} \left( \frac{1}{a_a} - \frac{2\sin\theta_H}{\lambda} \right) \right],$$

$$W_2 = \frac{1}{\sqrt{2}} \left[ \frac{a_a}{\sqrt{\lambda R_H}} - \sqrt{\lambda R_H} \left( \frac{1}{a_a} - \frac{2\sin\theta_H}{\lambda} \right) \right].$$

Using expression (26), ratio (34) can be represented as:

$$E_H^{(2)}(\theta_H) = N \left[ \int_0^{W_1} \exp\left(-i\frac{\pi}{2}g^2\right) dg + \int_0^{W_2} \exp\left(-i\frac{\pi}{2}g^2\right) dg \right]. \quad (35)$$

Both integrals in expression (35) were converted using Euler's formula:

$$\begin{aligned} \int_0^{W_1} \exp\left(-i\frac{\pi}{2}g^2\right) dg &= \int_0^{W_1} \cos\left(\frac{\pi}{2}g^2\right) dg - \\ &- i \int_0^{W_1} \sin\left(\frac{\pi}{2}g^2\right) dg, \end{aligned} \quad (36)$$

$$\begin{aligned} \int_0^{W_2} \exp\left(-i\frac{\pi}{2}g^2\right) dg &= \int_0^{W_2} \cos\left(\frac{\pi}{2}g^2\right) dg - \\ &- i \int_0^{W_2} \sin\left(\frac{\pi}{2}g^2\right) dg. \end{aligned} \quad (37)$$

In the final form, expression (32), applying ratio (30), (36), and (37):

$$E_H^{(2)}(\theta_H) = N \left\{ \left[ C\left(\frac{\pi}{2}W_1^2\right) + C\left(\frac{\pi}{2}W_2^2\right) \right] - \left[ -i \left[ S\left(\frac{\pi}{2}W_1^2\right) + S\left(\frac{\pi}{2}W_2^2\right) \right] \right] \right\}. \quad (38)$$

Based on the resulting expressions (31) and (38) that define the integrals that are included in expression (22), the latter is:

$$E_H(\theta_H) = E_0 b E_G(\theta_H) \frac{1}{2} \times \left\{ \begin{array}{l} M \left[ \begin{array}{l} C\left(\frac{\pi}{2} V_1^2\right) + C\left(\frac{\pi}{2} V_2^2\right) \\ -i \left[ S\left(\frac{\pi}{2} V_1^2\right) + S\left(\frac{\pi}{2} V_2^2\right) \right] \end{array} \right] + \\ + N \left[ \begin{array}{l} C\left(\frac{\pi}{2} W_1^2\right) + C\left(\frac{\pi}{2} W_2^2\right) \\ -i \left[ S\left(\frac{\pi}{2} W_1^2\right) + S\left(\frac{\pi}{2} W_2^2\right) \right] \end{array} \right] \end{array} \right\} \quad (39)$$

The ratio that defines the DD of the  $H$ -sectoral horn in the  $xOz$  plane takes the form:

$$F_H(\theta_H) = \frac{E_H(\theta_H)}{E_H^{\max}(0^0)} \quad (40)$$

Here, as above,  $F_G(\theta_H) = E_G(\theta_H)/E_G(0^0) = (1 + \cos\theta_H)/2$  is the normalized DD of a single Huygens emitter in the far zone [40].

**5. The results of the study of a horn antenna for electromagnetic field irradiation of sugar beet seeds**

**5. 1. Determining antenna parameters**

The far zone of the emitter is determined by the ratio  $L \geq 2a^2\lambda$  [39, 40]. Here  $a$  is the maximum size of the emitter in the plane under consideration.

According to expression (15), the phase of the field in the aperture of the  $H$ -sectoral horn is determined by the formula  $\psi = -\pi x^2/R_H$ . Maximum phase delay will occur at

the edges of the aperture horn at  $x = \pm a/2$ . At these points,  $\psi_{\max} = -\pi a^2/4\lambda R \geq -3\pi/4$  [42–44].

Hence we obtained the necessary ratio to determine the length of the sectoral horn in the plane of the vector  $\vec{H}$   $R_H \geq a^2/3\lambda$ . Since the aperture of the sectoral horn, considered in the plane of the vector  $\vec{E}$ , is equal to the cross section  $b$  of the standard rectangular waveguide of the four-millimeter range (1.8 mm). Then  $R_H$  and  $L$  will be uniquely determined by the aperture of the horn in the plane of the vector  $\vec{H}$ .

Before conducting numerical modeling, we considered the behavior of  $V_1$ ,  $W_1$  and  $W_2$ , which determined the limits of integration in expression (39) depending on  $h$ .

This is due to the fact that at different  $a_a$ ,  $R_H$ ,  $h$  and  $L$ ,  $V_1$ ,  $W_1$  and  $W_2$ , we could change the sign from positive to negative, which may eventually lead to distortion and misinterpretation of the DD of the  $H$ -sectoral horn.

Parameter  $V_2$  was not considered because it would be positive when changing  $a_a$ ,  $R_H$ ,  $h$  and  $L$ ,  $L$  within the limits below. Previous studies have shown that it is necessary to choose  $L = 200$  mm. Three values of the aperture of the horn  $a_a$  were considered (Fig. 3–5).

Fig. 3 shows the dependence of the parameter  $V_1$  on the width of the conveyor belt  $h$  for the three values of the aperture  $a_a$  of the  $H$ -sectoral horn.

Fig. 4 shows the dependence of the parameter  $W_1$  on the width of the conveyor belt  $h$  for the three values of the aperture  $a_a$  of the  $H$ -sectoral horn.

Fig. 5 shows the dependence of the parameter  $W_1$  on the width of the conveyor belt  $h$  for the three values of the aperture  $a_a$  of the  $H$ -sectoral horn.

In the plane of the vector  $\vec{H}$  at a frequency  $f = 74.0$  GHz ( $\lambda = 4.054$  mm) (Fig. 3–5):  $a_a = 20$  mm (the length of the horn is selected taking into account the above inequality,  $R_H = 35$  mm, curves 1);  $a_a = 30$  mm ( $R_H = 75$  mm, curves 2);  $a_a = 40$  mm ( $R_H = 35$  mm, curves 3). When constructing these plots, we moved from changes in the angle  $\theta_H$  to a change in the width of the conveyor belt  $h$ , using the expression  $\text{tg}\theta = h/L$ .

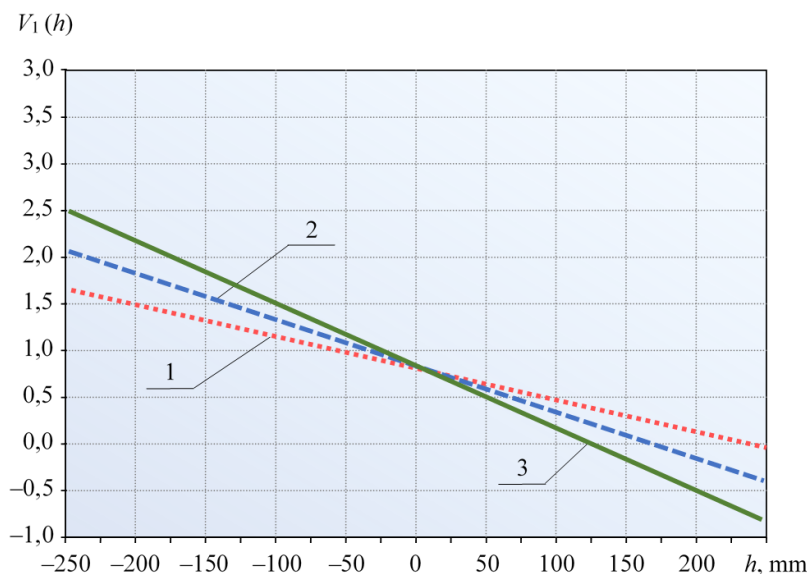


Fig. 3. Dependence of parameter  $V_1$  on the width of the conveyor belt  $h$  for the three values of the aperture  $a_a$  of the  $H$ -sectoral horn

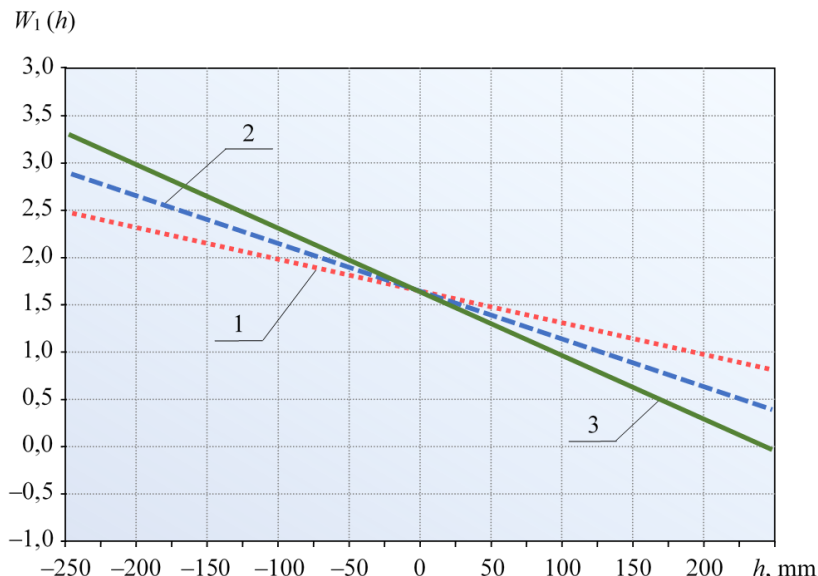


Fig. 4. Dependence of parameter  $W_1$  on the width of the conveyor belt  $h$  for three values of the aperture  $a_a$  of the  $H$ -sectoral horn

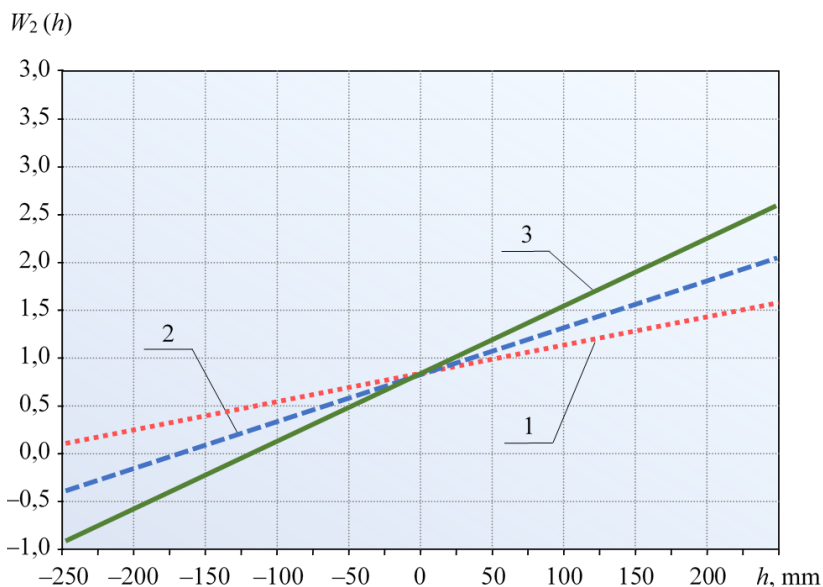


Fig. 5. Dependence of parameter  $W_2$  on the width of the conveyor belt  $h$  for three values of the aperture  $a_a$  of the  $H$ -sectoral horn

**5.2. Determining the power flow density and the height of the conveyor plane for irradiation of seeds with the electromagnetic field**

To determine the power flux density and the height of the conveyor plane, the DD of the considered emitter was analyzed (Fig. 6, 7) in the plane  $y0z$ .

Fig. 6 shows the directional diagram of the  $H$ -sectoral horn in the plane  $x0z$  with different sizes of the aperture  $a_a$ .

In this plane, the horn has a constant aperture, which was equal to the narrow side of the rectangular waveguide of the four-millimeter wavelength range ( $b=1.8$  mm). To build the DD, we used ratio (20).

Fig. 7 shows the DD of the considered horn emitter, built at the same values of the main parameters as the DD in

the  $x0z$  plane. Only the length to the plane of the conveyor belt changes:  $L=1200$  mm (curve 1);  $L=1000$  mm (curve 2);  $L=800$  mm (curve 3).

Determining the power level of radiation EM in the emitter aperture depends on the installation performance (300 kg/h), the area of the directional diagram, and the power flow density ( $100 \mu\text{W}/\text{cm}^2$ ).

The DD of the emitter is an ellipse with dimensions of semi-axes:  $a_e=127$  cm,  $b_e=21$  cm (Fig. 6, 7), and its area  $S=a_e\pi b_e=8000 \text{ cm}^2$ .

On an area of  $8000 \text{ cm}^2$  one can arrange seeds in one layer weighing 1.33 kg. In this case, the vector  $\vec{E}$  in the emitting apertures is normal to the direction of movement of sugar beet seeds along the conveyor.

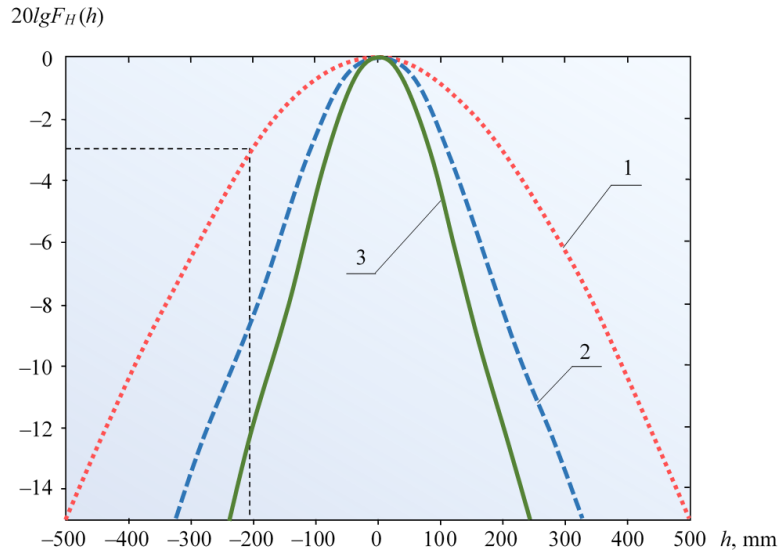


Fig. 6. Directional diagram of the *H*-sectoral horn in the plane *x0z* with different sizes of the aperture *a<sub>a</sub>*

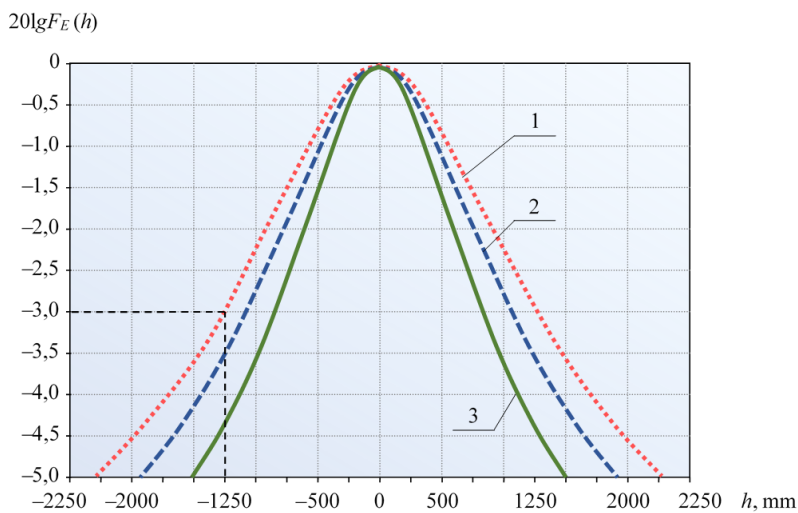


Fig. 7. Directional diagram of the *H*-sectoral horn in the *y0z* plane at different distances *L* to the observation plane

**5. 3. Determining the supplied power to the emitter horn and the speed of the conveyor**

To determine the power supplied to the emitter, we took the reflection coefficient from the irradiator equal to 1.8. This corresponds to the modulus of the reflection coefficient across the field  $|K|=0.286$ . The amount of power supplied to the emitter was determined from the following expression:

$$P_H = P_{inc}(1 - |K|^2), \tag{41}$$

where  $P_H = 0.8$  W.

The numerical calculation (41) showed that the value of the supplied power to one emitter is 0.87 W; accordingly, to two – 1.74 W.

**6. Discussion of results of the study of a horn antenna for electromagnetic field irradiation of sugar beet seeds**

As can be seen from Fig. 3–5, only at aperture  $a_a = 20$  mm, all three parameters  $V_1$ ,  $W_1$  and  $W_2$  have positive values in the specified change range of  $h$ .

Thus, as a result of the analysis, we obtained the magnitude of the aperture of the sectoral horn in the plane of the vector  $\vec{H}$  and the distance  $L$  at which it is necessary to determine the DD of the emitter in question.

Fig. 6 shows the proposed DDs of the *H*-sectoral horn, constructed in the plane *x0z* at a distance of  $L = 1200$  mm for the same dimensions of the aperture, which were considered above:  $a_a = 20$  mm (curve 1);  $a_a = 30$  mm (curve 2);  $a_a = 40$  mm (curve 3). When constructing DD using expression (40), it was taken into account, as above, that  $tg\theta_H = h/L$ .

The above DDs in Fig. 7 demonstrate that the aperture, which is equal to 20 mm (curve 1), provides overlapping of the conveyor belt at the level of half power (–3 dB). In this case, the width of DD is 420 mm.

With an increase in the aperture of the horn (Fig. 6, curves 2, 3), the width of DD narrows.

From the analysis of Fig. 6, 7 we can conclude that the DD of the emitter is an ellipse with dimensions of semi-axes:  $a_e = 127$  cm,  $b_e = 21$  cm, and area  $S = 8000$  cm<sup>2</sup>. On such a plane, seeds can fit in one layer weighing 1.33 kg.

With a power in the aperture of the antenna of the emitter of 0.8 W and an exposure of 33 s in 1 hour, 145 kg of sugar beet seeds can be irradiated.

For seed treatment weighing 300 kg per 1 hour, with an exposure of 33 s and a power flow density of  $100 \mu\text{W}/\text{cm}^2$ , it is necessary to increase the working surface of the conveyor to  $16000 \text{ cm}^2$ , and at a height of 1200 mm from the conveyor band to place two emitting  $H$ -sectoral horns located at a distance of 2540 mm from each other.

Fig. 7 shows that with increasing distance  $L$ , the width of DD will increase. With a distance to the observation plane equal to 1200 mm, the width of the directional diagram at the level of half the power ( $-3 \text{ dB}$ ) along the direction of movement of the conveyor is 2540 mm.

For presowing treatment of sugar beet seeds, on the basis of theoretical studies, a prototype of a  $H$ -sectoral antenna was made.

To determine the level of radiation power from the aperture of the  $H$ -sector horn, the reflection coefficient from the emitter loaded on free space is given. For this purpose, a panoramic meter was used for a voltage standing wave ratio (VSWR) and a standard measurement scheme. We received VSWR 1.8 at frequency  $f=74 \text{ GHz}$ . This corresponds to the module of the reflection coefficient for the field of 0.286. The level of power emitted from the aperture of the sectoral horn was determined from equation (41).

We received DD of the sectoral horn at a distance of  $L=1200 \text{ mm}$  from the aperture plane. Based on the studies performed, the  $H$ -sectoral horn was made, which has the following geometric dimensions:  $a_a=20 \text{ mm}$ ,  $R_H=35 \text{ mm}$ ,  $b=1.8 \text{ mm}$ . The study was conducted at a frequency of  $f=74.0 \text{ GHz}$ . Flowchart of the measuring bench consisted of transmission and receiving tracts. The transmission tract includes a semiconductor generator with a power supply;  $p$ - $i$ - $n$  modulator, which is supplied with a sinusoidal signal at a frequency of 1 kHz from a low-frequency generator (G3-102); installation attenuator and  $H$ -sector horn antenna.

The modulator was turned on to the tract to expand the dynamic range of the measured signals. The circuit provides an additional channel for controlling the amplitude and frequency of the signal of the semiconductor generator. Therefore, the experimental installation included a directional branch; polarization attenuator; resonant wavemeter; detector section; selective amplifier (U2-8); two-beam oscilloscope (C1-83). To eliminate possible rereflection, in the tract in the second arm of the directed branch included an agreed load.

The composition of the receiving tract included a measuring probe; polarization attenuator; detector section; selective amplifier, the signal from the output of which is fed to the second input channel of the oscilloscope. Since studies were carried out at a great distance from the emitter ( $L=1200 \text{ mm}$ ), a pyramidal horn with an aperture dimension of  $20 \times 10 \text{ mm}$ , which has an integrating characteristic, was used to expand the dynamic range of signals received as a measuring probe. The entire receiving tract is assembled on a movable platform that can move in 1 mm increment.

The studies were carried out precisely in the plane  $x0z$  because in the plane  $y0z$  the width of DD of the studied sectoral horn in terms of half power should exceed 2.5 m and its measurement under laboratory conditions causes certain difficulties. It is determined that the maximum difference between the measured and calculated DDs of the  $H$ -sectoral horn of the above geometric dimensions does not exceed 12 %.

This suggests that in practice the width of DD of the emitter under study in the plane  $y0z$  in terms of half power level will be approximately 2.5 m. Knowing the dimensions of DD of the considered  $H$ -sectoral horn in the plane of the conveyor belt on which the seed is located, we determined the flux density of the incident power in this plane.

Since we considered the width of DD of the sectoral horn in two mutually perpendicular planes at the level of half power, considering that there are no power losses in free space, we determined the level of incident power in the plane of the conveyor belt. DD for one emitter is an ellipse with dimensions of semi-axes  $a_e=127 \text{ cm}$ ,  $b_e=17.5 \text{ cm}$ , and its area  $S=a_e \pi b_e=7000 \text{ cm}^2$ .

The power at the output of the emitter should be 0.7 watts. Thus, in order to obtain a power flow density of about  $100 \mu\text{W}/\text{cm}^2$  in the conveyor plane, it is necessary to place two emitting  $H$ -sectoral horns above it at a distance of 1200 mm, located at a distance of 2540 mm from each other, for a conveyor speed of 15 cm/s. At the same time, the vector  $\vec{E}$  in the emitting apertures is parallel to the direction of movement of the seeds by the conveyor. Power level supplied to the sectoral horns is defined from equation (41); it is equal to 1.52 watts.

Since we have two field spots along the direction of movement of the seeds, the total length will be 508 cm and, dividing it by 33, we get the speed of the conveyor  $\approx 15 \text{ cm/s}$ .

The results of our study confirmed that the use of a sectoral horn antenna in comparison with the existing designs of devices for presowing seed treatment with a low-energy electromagnetic field makes it possible to more efficiently provide the necessary values of the biotropic parameters of the electromagnetic field of irradiated seeds during flow processing. At the same time, well-known designs of irradiation installations use slit emitters [45] and resonator chambers [46, 47], which demonstrate a dependence of geometric dimensions on the wavelength, and, accordingly, cannot provide high-quality DD and uniformity of power flux density if it is necessary to change the biotropic parameters of the electromagnetic field.

The limitations in the studies were as follows. The frequency properties of the horn antenna in our case depended on the properties of not only the horn itself but also the waveguide. The operating frequency range of the waveguide was limited by the condition for the propagation of the main type of wave in it:

$$\lambda^{(2)} < \lambda < \lambda^{(1)},$$

where  $\lambda^{(1)}$  is the critical wavelength of the main type ( $H_{10}$  and  $H_{11}$  for rectangular and round waveguides, respectively);  $\lambda^{(2)}$  is the critical wavelength of the first higher type.

Rectangular waveguides allowed approximately one and a half overlap over the wave range, namely,  $\lambda_{\min} \geq 1.1a$  and  $\lambda_{\max} \geq 1.67b$ . Provided that round waveguides are used, the operating frequency range is somewhat smaller.

Since the cross section of the horn is larger than in the waveguide, the above limitation did not exist for it, however, with the change in wavelength, the relative dimensions of the horn aperture and the maximum phase error, and, consequently, the directional coefficient (DC) of the antenna, changed. The parameters that determined the operating frequency band of the horn antenna, in this case, revealed directional properties (width of the main petal DD, level of side petals), or DC. It was believed that with a one-and-a-half overlapping coefficient, which was provided by a supply waveguide, the change in DC slightly exceeded 20 %.

The total reflections in the waveguide were determined both by the waves reflected from the aperture of the horn and by the waves reflected from the place where the waveguide passed into the horn (neck). The latter were not taken into account in the calculations.

The reflection was taken into account only for the calculation of power, its impact on the distortion of DD is not indicated. The calculation of power did not take into account the loss of power on the side lobes.

According to the results of research, it is possible to create a base of geometric presets for adjusting installations for different types of seeds, the desired performance, the structural features of installations, and existing emitters.

## 7. Conclusions

1. For electromagnetic field irradiation of sugar beet seeds for presowing treatment with a frequency of 73...75 GHz in a continuous flow, one should use an *H*-sectoral horn emitter with parameters – aperture width  $a_a=20$  mm; horn length  $R_H=35$  mm;  $b=1.8$  mm.

2. For irradiation of sugar beet seeds on the conveyor plane with a power flow density of  $P=100 \mu\text{W}/\text{cm}^2$  it is nec-

essary to place two horns at a distance of 1200 mm above the conveyor at a distance of 2540 mm from each other.

3. Treatment of sugar beet seeds with electromagnetic radiation in a continuous flow with a capacity of 300 kg/h is possible with a power of up to 2 W, which is supplied to two horn antennas, the speed of the conveyor is  $\approx 15$  cm/s.

## Conflicts of interest

The authors declare that they have no conflicts of interest in relation to the current study, including financial, personal, authorship, or any other, that could affect the study and the results reported in this paper.

## Funding

The study was conducted without financial support.

## Data availability

All data are available in the main text of the manuscript.

## References

- Huyghe, C., Desprez, B., Laudinat, V. (2020). Sugar beet. *Quae*. doi: <https://doi.org/10.35690/978-2-7592-3185-0>
- Hruzynska, I., Smahina, A., Airapetov, M., Zhyhadlo, V. (2018). Zelena knyha "Rehuliuвання rynku tsukru". Ofis efektyvnoho rehuliuвання. Available at: [https://issuu.com/office\\_brdo/docs/\\_\\_\\_\\_\\_?utm\\_medium=referral&utm\\_source=regulation.gov.ua](https://issuu.com/office_brdo/docs/_____?utm_medium=referral&utm_source=regulation.gov.ua)
- Abbott, G. C. (2020). *Sugar*. Routledge, 414. doi: <https://doi.org/10.4324/9781003292203>
- Fyliuk, G., Sytenko, D. (2014). Causes of crisis situation in Ukraine sugar industry enterprises and their solutions. *Bulletin of Taras Shevchenko National University of Kyiv. Economics*, 158, 6–11. Available at: [http://bulletin-econom.univ.kiev.ua/wp-content/uploads/2015/11/158\\_6-11.pdf](http://bulletin-econom.univ.kiev.ua/wp-content/uploads/2015/11/158_6-11.pdf)
- Smit, A. B., Jongeneel, R. A., Prins, H., Jager, J. H., Hennen, W. H. G. J. (2017). Impact of coupled EU support for sugar beet growing: more production, lower prices. *Wageningen Economic Research*. doi: <https://doi.org/10.18174/430039>
- Mitchell, D. (2004). *Sugar Policies: Opportunity for Change*. Washington.
- Kosulina, N. G., Cherenkov, A. D. (2008). Low-energy electromagnetic technologies are in plantgrower. *Svitlotekhnika ta elektroenerhetyka*, 4, 80–85. Available at: <http://eprints.kname.edu.ua/8430/1/80-85.pdf>
- Chernaya, M. A., Kosulina, N. G., Avrunin, O. G. (2013). Analiz problem predposevnoy obrabotki semyan na osnove elektromagnitnykh tekhnologiy. *Visnyk Kharkivskoho natsionalnoho tekhnichnoho universytetu silskoho hospodarstva im. Petra Vasylenka*, 141, 93–94.
- Tanaš, J., Cherenkov, A. D., Kosulina, N. G., Yaroslavskyy, Y. I., Titova, N. V., Aizhanova, A. (2018). Justification of the electromagnetic impulse method destruction of insect pests in gardens. *Photonics Applications in Astronomy, Communications, Industry, and High-Energy Physics Experiments 2018*. doi: <https://doi.org/10.1117/12.2501665>
- Mykhaylova, L., Ryd, A., Potapski, P., Kosulina, N., Cherenkov, A. (2018). Determining the electromagnetic field parameters to kill flies at livestock facilities. *Eastern-European Journal of Enterprise Technologies*, 4 (5 (94)), 53–60. doi: <https://doi.org/10.15587/1729-4061.2018.137600>
- Kosulina, N., Kosulin, S. (2022). Determination of biotropic parameters of a pulsed electric field for increasing immunoglobulins in cow coloster. *Sciences of Europe*, 103, 90–93.
- Kosulina, N., Kosulin, S. (2022). Application of low-energy radio-wave emissions in medicine and animal husbandry. *The scientific heritage*, 99, 22–25. Available at: <https://ru.calameo.com/read/00505976992f912ada90e>
- Uğurlu, B. T. (2022). On the wave nature of particles. *Physics Essays*, 35 (2), 171–174. doi: <https://doi.org/10.4006/0836-1398-35.2.171>
- Rossing, T. D., Chiaverina, C. J. (2019). The Wave Nature of Light. *Light Science*, 25–49. doi: [https://doi.org/10.1007/978-3-030-27103-9\\_2](https://doi.org/10.1007/978-3-030-27103-9_2)
- Kuchin, L. F., Cherenkov, A. D., Kosulina, N. G. (2002). Znachenie strukturnoy organizatsii bioobjektov pri vzaimodeystvii s nizkoenergeticheskimi polarizovannymi elektromagnitnymi polyami. *Pratsi. Tavriyska derzhavna ahrotekhnichna akademiya*, 6, 26–29.
- Kosulina, N. H. (2003). Vykorystannia mikrokhvylovykh tekhnolohiy u silskomu hospodarstvi. *Pratsi. Tavriyska derzhavna ahrotekhnichna akademiya*, 15, 141–148.

17. Cherenkov, A. D., Kosulina, N. G. (2005). Primenenie informatsionnykh elektromagnitnykh poley v tekhnologicheskikh protsessakh sel'skogo khozyaystva. *Svitlotekhnika ta elektroenerhetyka*, 5, 77–80.
18. Kosulina, N. H., Cherenkov, O. D. (2005). Doslidzhennia vplyvu elektromagnitnoho polia na nasinnia soi. *Visnyk Kharkivskoho derzhavnogo tekhnichnoho universytetu silskoho hospodarstva*, 37 (1), 152–160.
19. Kosulina, N. G. (2006). Opredelenie diapazona izmeneniy parametrov elektromagnitnogo polya, vozdeystvuyuschikh na semena soi. *Tavriyska derzhavna ahrotekhnichna akademiya. Pratsi*, 35, 102–105.
20. Popriadukhin, V., Popova, I., Kosulina, N., Cherenkov, A., Chorna, M. (2017). Analysis of the electromagnetic field of multilayered biological objects for their irradiation in a waveguide system. *Eastern-European Journal of Enterprise Technologies*, 6 (5 (90)), 58–65. doi: <https://doi.org/10.15587/1729-4061.2017.118159>
21. Konstantinov, I. S., Mamatov, A. V., Sapryka, V. A., Sapryka, A. V., Kosulina, N. G. (2015). Theoretical analysis of electromagnetic field electric tension distribution in the seeds of cereals. *Research Journal of Pharmaceutical, Biological and Chemical Sciences*, 6 (6), 1686–1694.
22. Olenyuk, A. A. (2013). Calculation of EMF resonance frequency for presowing processing of sugar beet seeds. *Eastern-European Journal of Enterprise Technologies*, 1 (9 (61)), 13–16. Available at: <http://journals.uran.ua/eejet/article/view/9494>
23. Olenyuk, A. A. (2012). Opredelenie rezonansnoy chastoty EMP dlya vozdeystviya na semena sfericheskoy formy. *Visnyk natsionalnoho tekhnichnoho universytetu «KhPI»*, 66 (972), 173–177.
24. Cherenkov, A. D., Kosulina, N. G., Sereda, A. I. (2004). Analiz rozpodilu elektromagnitnoho polia formovanoho anteny pry stroiamy dlia vplyvu na biolohichni obiekty. *Visnyk Kharkivskoho derzhavnogo tekhnichnoho universytetu silskoho hospodarstva*, 27 (1), 238–245.
25. Josefsson, L., Rengarajan, S. (Eds.) (2018). *Slotted waveguide array antennas: theory, analysis and design*. The Institution of Engineering and Technology, 400.
26. Yang, F., Rahmat-Samii, Y. (2008). Surface wave antennas. *Electromagnetic Band Gap Structures in Antenna Engineering*, 203–237. doi: <https://doi.org/10.1017/cbo9780511754531.008>
27. Kobayashi, H. (2020). Horn Antenna. *Analyzing the Physics of Radio Telescopes and Radio Astronomy*, 144–177. doi: <https://doi.org/10.4018/978-1-7998-2381-0.ch008>
28. Kosulina, N. G., Korshunov, K. S. (2021). Calculation of a specialized antenna for biological research. *Engineering of nature management*, 22, 99–103. Available at: <https://repo.btu.kharkov.ua/bitstream/123456789/1211/1/16.pdf>
29. Volakis, J. L. (2019). *Antenna engineering handbook*. McGraw Hill, 1424.
30. Waterhouse, R. B. (2005). *Traveling Wave Antennas*. *Encyclopedia of RF and Microwave Engineering*. doi: <https://doi.org/10.1002/0471654507.em466>
31. Chand, R. K., Raghavendra, M. V., Sathyavathi, K. (2013). Radiation Analysis and Design of Pyramidal Horn Antenna. *International Journal Of Engineering Research & Technology (IJERT)*, 2 (10). Available at: <https://www.ijert.org/research/radiation-analysis-and-design-of-pyramidal-horn-antenna-IJERTV2IS100033.pdf>
32. Hirokawa, J., Zhang, M. (2015). Waveguide Slot Array Antennas. *Handbook of Antenna Technologies*, 1–21. doi: [https://doi.org/10.1007/978-981-4560-75-7\\_51-1](https://doi.org/10.1007/978-981-4560-75-7_51-1)
33. Balanis, C. A. (2016). *Antenna Theory: Analysis and Design*. Hoboken. John Wiley and Sons, 1104.
34. Kildal, P.-S. (2015). *Foundations of antenna engineering: a unified approach for line-of-sight and multipath*. Artech.
35. Olver, A. D. (1992). *Microwave and Optical Transmission*. Wiley, 400.
36. Kong, J. A. (1994). *Electromagnetic Wave Theory*. Wiley.
37. Towne, D. H. (1998). *Wave Phenomena*. Dover Publications.
38. Elmore, W. C., Heald, M. A. (1995). *Physics of Waves*. Dover Publications.
39. Wieglofer, W. S., Lakhtakia, A. (Eds.) (2003). *Introduction to Complex Media for Optics and Electromagnetics*. SPIE. doi: <https://doi.org/10.1117/3.504610>
40. Yanke, E. (1994). *Spetsial'nye funktsii (Formuly, grafiki, tablitsy)*. Kyiv: Naukova dumka, 344.
41. Dass, H. K. (2007). *Advanced Engineering Mathematics*. S Chand & Co Ltd, 1136.
42. Godon Webster, A. (2016). *Partial Differential Equations of Mathematical Physics*. Dover Publications, 464.
43. Riley, K. F., Hobson, M., P. Bence, S. J. (2012). *Mathematical Methods for Physics and Engineering*. Cambridge University Press, 1333. doi: <https://doi.org/10.1017/cbo9781139164979>
44. Freedden, W., Gutting, M. (2013). *Special Functions of Mathematical (Geo-)Physics*. Springer, 501. doi: <https://doi.org/10.1007/978-3-0348-0563-6>
45. Kalinin, L. H., Moiseev, V. F., Malinovskiy, V. V. (2006). Pat. No. 19550 UA. Microwave device for presowing seed treatment. No. u200607446; declared: 04.07.2006; published: 15.12.2006. Available at: <https://uapatents.com/2-19550-mikrokhvilovijj-pristriij-peredposivno-obrobki-nasinnya.html>
46. Dziuba, V. P., Kalinin, L. H., Tuchnyi, V. P., Tokovenko, O. M. (2003). Pat. No. 53954 UA. Microwave device for presowing seed treatment. No. 2002032451; declared: 28.03.2002; published: 17.02.2003. Available at: <https://uapatents.com/2-53954-mikrokhvilovijj-pristriij-doposivno-obrobki-nasinnya.html>
47. Sydoruk, Y. K. (2011). Pat. No. 65629 UA. Microwave device for presowing seed treatment, drying grain and other loose materials. No. u201106351; declared: 20.05.2011; published: 12.12.2011. Available at: <https://uapatents.com/4-65629-mikrokhvilovijj-pristriij-dlya-peredposivno-obrobki-nasinnya-sushinnya-zerna-ta-inshikh-sipuchikh-materialiv.html>